Ca^{2+} Binding Protein Frequenin Mediates GDNF-Induced Potentiation of Ca^{2+} Channels and Transmitter Release

Chang-Yu Wang,[1,2,4] Feng Yang,[1,4]
Xiangping He,[1] Ana Chow,[1] Jing Du,[1]
James T. Russell,[1] and Bai Lu[1,3]
[1] Laboratory of Cellular
  and Synaptic Neurophysiology
National Institute of Child Health
  and Human Development
National Institutes of Health
Bethesda, Maryland 20892
[2] Genetics Graduate Program
George Washington University
Washington DC, 20052

Summary

Molecular mechanisms underlying long-term neuro-trophic regulation of synaptic transmission and plas-ticity are unknown. We report here that long-term treatment of neuromuscular synapses with glial cell line-derived neurotrophic factor (GDNF) potentiates spontaneous and evoked transmitter release, in ways very similar to presynaptic expression of the Ca^{2+} bind-ing protein frequenin. GDNF enhances the expression of frequenin in motoneurons, and inhibition of freque-nin expression or activity prevents the synaptic action of GDNF. GDNF also facilitates Ca^{2+} influx into the nerve terminals during evoked transmission by en-hancing Ca^{2+} currents. The effect of GDNF on Ca^{2+} currents is blocked by inhibition of frequenin expres-sion, occluded by overexpression of frequenin, and is selective to N-type Ca^{2+} channels. These results identify an important molecular target that mediates the long-term, synaptic action of a neurotrophic factor.

Introduction

Changes in the efficacy of synaptic transmission, also known as synaptic plasticity, are thought to be the cellu-lar mechanisms for the development and function of the nervous system, as well as for complex behaviors such as learning and memory. Recent studies have identified neurotrophins as a new class of neuromodulators for synaptic plasticity in the central and peripheral nervous systems (CNS and PNS) (Lu and Chow, 1999; McAllister et al., 1999). For example, application of brain-derived neurotrophic factor (BDNF) or neurotrophin-3 (NT3) to the neuromuscular junction (NMJ) elicits a rapid en-hancement of transmitter release (Lohof et al., 1993; Stoop and Poo, 1995). The synthesis of NT3 and secre-tion of neurotrophin-4 (NT4) from the postsynaptic mus-cle cells increase rapidly in response to presynaptic activity (Wang and Poo, 1997; Xie et al., 1997). The acute effect of neurotrophins occurs preferentially to active synapses (Boulanger and Poo, 1999). Moreover, such regulation requires a cascade of protein phosphoryla-

tion events (He et al., 2000; Yang et al., 2001) and is independent of new protein synthesis (Stoop and Poo, 1995; Chang and Popov, 1999). In the hippocampus, substantial evidence indicates that BDNF acutely facili-tates long-term potentiation (LTP) (Korte et al., 1995; Figurov et al., 1996; Patterson et al., 1996). This effect is due primarily to a presynaptic mechanism (Gottschalk et al., 1998; Xu et al., 2000) and has been attributed to a potentiation of synaptic responses to tetanic stimulation and an enhancement of synaptic vesicle docking, possi-bly through changes in the levels and/or phosphoryla-tion of synaptic proteins (Gottschalk et al., 1999; Pozzo-Miller et al., 1999; Jovanovic et al., 2000).

In addition to their acute effects on synaptic transmis-sion and plasticity, neurotrophins also exhibit a long-term regulatory role in synapse development and func-tion. Long-term application of neurotrophins exerts complex modulation of dendritic and axonal growth in the brain, particularly in the visual system (McAllister et al., 1995; Cohen-Cory and Fraser, 1996). Neurotrophins are involved in activity-dependent synaptic competition and formation of ocular dominance columns in the visual cortex (Maffei et al., 1992; Cabelli et al., 1995). Substan-tial evidence suggests that neurotrophins promote the maturation of NMJ in vitro and in vivo (Wang et al., 1995; Liou and Fu, 1997; Gonzalez et al., 1999; Nick and Ribera, 2000). Long-term regulation of synaptic trans-mission by neurotrophins has also been observed in the CNS (Rutherford et al., 1998; Vicario-Abejon et al., 1998). While long-term regulation of synapses by neurotroph-ins is widely observed, virtually nothing is known about its underlying molecular mechanisms.

In an attempt to investigate whether neurotrophic reg-ulation of synapses is a general biological process, we have studied the effect of GDNF on synaptic transmis-sion at NMJ. GDNF belongs to a newly identified family of neurotrophic factors (Lin et al., 1993) whose functions are mediated by a two-component receptor complex: a signaling component called c-RET which is a receptor tyrosine kinase, and a ligand binding component called GFR-α (Baloh et al., 2000). Several lines of evidence suggest that GDNF supports the survival and differentia-tion of motoneurons (Henderson et al., 1994; Oppenheim et al., 1995; Yan et al., 1995). GDNF is expressed in the muscle and Schwann cells and is retrogradely trans-ported by motoneurons, which express GDNF receptors GFR-α1 and c-RET (Pachnis et al., 1993; Henderson et al., 1994; Yan et al., 1995; Treanor et al., 1996). Trans-genic mice overexpressing GDNF in muscles exhibit hyperinnervation at the NMJ (Nguyen et al., 1998). Little is known, however, about whether GDNF regulates the function of the neuromuscular synapses, in addition to its role in enhancing survival or promoting neurite out-growth of developing motoneurons.

In a recent study, chronic treatment of cultured mid-brain dopaminergic neurons with GDNF has been shown to increase the release of glutamate, a cotransmitter in these neurons (Bourque and Trudeau, 2000). Molecular mechanisms for the long-term synaptic effects of GDNF and, indeed, those for any neurotrophic factors remain

[3] Correspondence: lub@codon.nih.gov
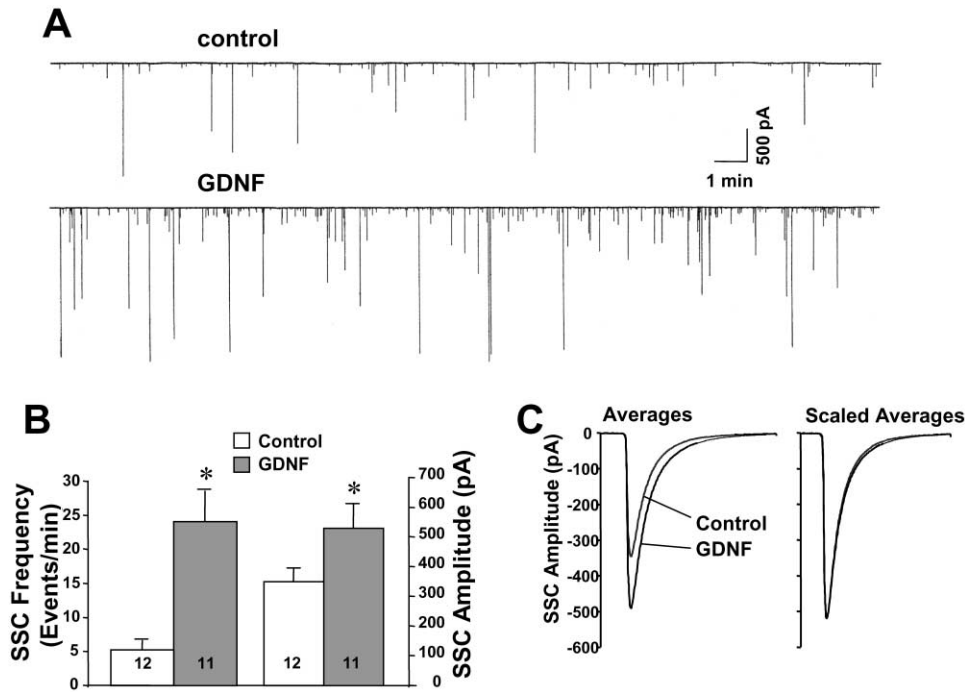[4] These authors contributed equally to this work.

Figure 1. Effects of GDNF on Spontaneous Synaptic Currents

More than 100 SSC events were recorded for each synapse, analyzed by the SCAN program or averaged to obtain a single waveform. (A) Examples of SSCs recorded from control and GDNF-treated synapses in 1-day-old cultures. SSCs of varying amplitudes are shown as downward deflections (Vh = −70mV, filtered at 150 Hz). (B) Summary of GDNF effects on mean SSC frequency and amplitude. Unless indicated otherwise, the data in this and all other figures are mean ± SEM obtained from synapses treated with or without GDNF (40 pM) for 1 day. The number associated with each column is the number of recordings performed, and the data were subjected to student's t test. *: p < 0.05. (C) Lack of effect of GDNF on SSC rise and decay times. Waveforms from control (n = 9) and GDNF-treated (n = 10) synapses were averaged (left) and then scaled (right) for comparison.

unknown. It is unclear what the molecular targets of specific neurotrophic factors are or how these molecules act to regulate synaptic transmission. In the present study, we address this issue using the *Xenopus* nerve-muscle coculture. Our experiments demonstrate that GDNF elicits a long-term modulatory effect on synaptic transmission at NMJ and that this effect is mediated by an upregulation of the expression of the neuronal Ca^{2+} binding protein frequenin. Further, we show that GDNF/frequenin facilitates synaptic transmission by enhancing Ca^{2+} channel activity, leading to an enhancement of Ca^{2+} influx. Thus, this study has identified a molecular target that mediates the long-term synaptic action of a neurotrophic factor.

Results

Long-Term Facilitation of Synaptic Transmission by GDNF

To determine the role of GDNF in synaptic transmission, we performed whole-cell, voltage-clamp recordings of spontaneous synaptic currents (SSCs) at the neuromuscular synapses in culture (Wang et al., 1995). The SSCs represent spontaneous secretion of individual acetylcholine (ACh)-containing vesicles from motor nerve terminals independent of action potentials. Acute application of GDNF (up to 1 hr, 0.4 nM) to the NMJ failed to elicit any changes in SSCs (data not shown). In contrast,

long-term treatment with GDNF (1 day, 40 pM, in all experiments) dramatically increased the frequency of SSCs (Figures 1A and 1B). On average, SSC frequency in GDNF-treated synapses increased 5-fold as compared with that in control synapses. Since SSC frequency reflects the rate of vesicle fusion spontaneously at the presynaptic terminals, these results suggest a presynaptic action of GDNF. A small but significant increase in the mean amplitude of SSCs was also observed in neurons treated with GDNF (Figures 1B and 1C). This could be due to the lengthening of ACh channel open time, as reflected by SSC decay time (Wang and Poo, 1997). However, treatment with GDNF did not affect SSC decay time (control: 12.6 ± 8.0 ms; GDNF: 13.3 ± 3.1 ms; p > 0.1, t test). Scaling of averaged SSCs in control and GDNF-treated synapses shows that the two traces almost superimpose on each other (Figure 1C), arguing against a change in ACh channel open time. It is possible that GDNF has a small effect on the number of ACh receptors at the NMJ.

We next examined the role of GDNF in functional synaptic transmission by recording evoked synaptic currents (ESCs). Treatment with GDNF resulted in a 2-fold increase in the amplitude of ESCs. To test whether GDNF affects probability of transmitter release (Pr), we measured paired-pulse facilitation (PPF), the increase in the second ESC amplitude when a synapse is activated by two successive presynaptic stimuli. PPF is believed to
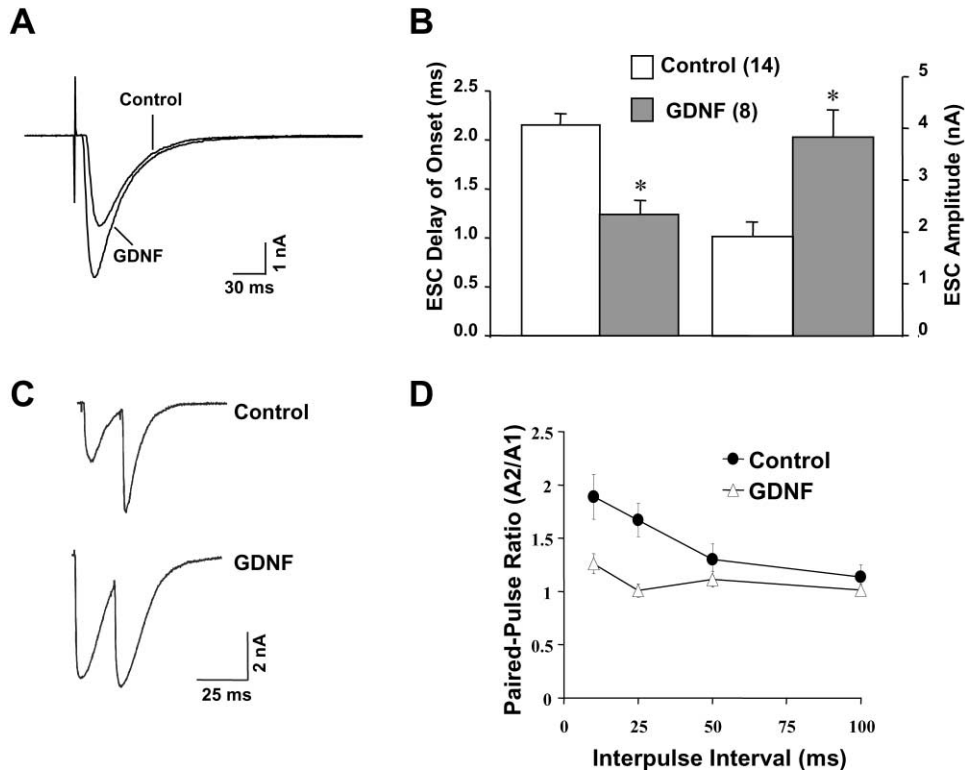
Figure 2. Effects of GDNF on Evoked Synaptic Currents

(A) Examples of ESCs from control and GDNF-treated synapses. (B) Summary of GDNF effects on ESC amplitude and synaptic delay (interval between stimulation artifact and the beginning of ESC). (C) Examples of paired-pulse facilitation (PPF), elicited by twin pulses with a 25 ms interval. GDNF treatment results in an increase in the amplitude of the first ESC but a decrease in the ratio of second (A2) and first (A1) ESCs. (D) PPF ratio curves showing facilitation at various interpulse intervals. n = 7–15 for control; n = 15–20 for GDNF-treated synapses. GDNF significantly increases PPF ratios at 10 and 25 ms interpulse intervals.

reflect an enhancement of transmitter release resulting from changes in residual terminal Ca^{2+}, and manipulations that increase Pr usually decrease the magnitude of PPF (Zucker, 1989). Whereas treatment with GDNF increased the first ESC amplitude, the ratio of the second and the first amplitudes (A2/A1) was significantly reduced, particularly at shorter interpulse interval (Figures 2C and 2D, 10 and 25 ms).

To further characterize the presynaptic effects of GDNF, we used FM dye destaining, a measure of transmitter release independent of postsynaptic cells (Ryan et al., 1993). Figure 3A shows the phase images of a myocyte innervated by a motoneuron. The strong fluorescence spot on the myocyte represents a typical dye-loaded presynaptic bouton (Figure 3B). The fluorescence images were quite stable in wash solutions over a period of 10 min with minimum bleaching (data not shown). Transmitter release was initiated by rapid perfusion of high K^+ destaining solution containing the same $[Ca^{2+}]_o$ as the wash solution. In normal $[Ca^{2+}]_o$ (2 mM), more than 95% of the dye fluorescence almost disappeared within 3 min after the perfusion of high K^+ destaining solution (Figure 3C; see also Supplemental Movie S1 at http://www.neuron.org/cgi/content/full/32/1/99/DC1). Change in $[Ca^{2+}]_o$ is known to alter Pr. The rate of FM dye destaining, which represents the amount of transmitter release per unit time, became slower with decreasing $[Ca^{2+}]_o$ (Figure 3D), suggesting that changes

in the destaining rate reflect the changes in Pr. At 2 mM, 0.5 mM, and 0.1 mM of $[Ca^{2+}]_o$, the time constant (τ) was 43.8 $\pm$ 7.0 s, 78.8 $\pm$ 10.8 s, and 270.6 $\pm$ 46.7 s, respectively (Figure 3E). In cultures treated with GDNF, FM dye destaining became faster (Figure 3E), mimicking the effect of increasing $[Ca^{2+}]_o$. Moreover, the effect of GDNF was much greater when $[Ca^{2+}]_o$ was reduced from 2 mM to 0.1 mM, indicating that GDNF enhances transmitter release more effectively when Pr is low. However, the total amounts of transmitter release in normal $[Ca^{2+}]_o$ (2 mM), as reflected by the difference in fluorescence intensity before and 2 min after application of high K^+ destaining solution (ΔF), were quite similar in control (ΔF = 95.1% $\pm$ 2.0%) and GDNF-treated (ΔF = 99.1% $\pm$ 1.2%) synapses. Taken together, these results imply that GDNF regulates transmitter release primarily by increasing Pr.

To begin to ascertain how GDNF enhances transmitter release, we examined whether it affects synaptic delay, the time interval between action potential firing and ESC generation. Synaptic delay includes the time for an action potential to travel from cell body to the nerve terminal, plus the time from Ca^{2+} channel opening to transmitter release (Llinas, 1982). In control neurons, the action potential travel time in a 50–100 μm long axon was less than 0.5 ms (see also Yazejian et al., 1997), but the synaptic delay was 2.2 ms (Figure 2B). Thus, action potential travel time accounts for only a small proportion
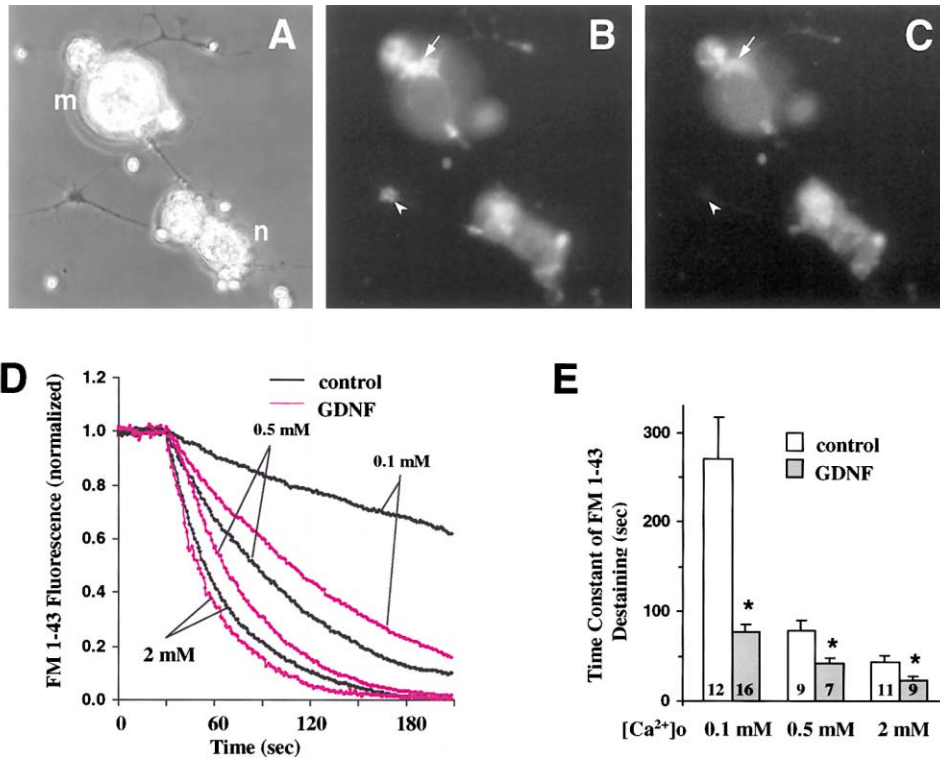
Figure 3. Effects of GDNF on FM1-43 Destaining

(A) Phase image of a myocyte (m) innervated by a motoneuron (n). (B) Fluorescence image of the same field after loading of FM1-43 dye by high K^{+} loading solution. Arrow indicates a fluorescence spot at the NMJ, and arrowhead indicates one at a free nerve terminal. (C) Same as (B) but after application of high K^{+} destaining solution containing 2 mM $[Ca^{2+}]_o$. (D) Averaged destaining curves. After FM1-43 loading, the cells were rinsed extensively with wash solutions containing different $[Ca^{2+}]_o$, as indicated. Destainings were initiated by perfusing high K^{+} destaining solution with $[Ca^{2+}]_o$ matching the wash solution. (E) Summary of GDNF effects on the rate of destaining in different $[Ca^{2+}]_o$. The destaining time courses of individual fluorescent synaptic boutons were fitted by single exponential curves, and the time constant (τ) was obtained for each bouton. The mean destaining time constant in a particular condition was then obtained by averaging τ from all synapses.

of synaptic delay. Treatment with GDNF reduced synaptic delay by half (Figures 2A and 2B), suggesting that GDNF significantly increases the efficiency of excitation-secretion coupling rather than shortening the action potential travel time.

GDNF Enhances Frequenin Expression in Motoneurons

A reduction in synaptic delay is rarely seen at these synapses but has been observed when the Ca^{2+} binding protein frequenin is overexpressed in the presynaptic motoneurons (Olafsson et al., 1995). Frequenin (also called neuronal calcium sensor-1 or NCS-1) is a neural-specific protein known to facilitate synaptic transmission at the NMJ (Pongs et al., 1993). At *Xenopus* NMJ, frequenin is expressed in presynaptic motoneurons but not in postsynaptic muscle cells, and overexpression of frequenin in motoneurons elicits changes almost identical to those induced by GDNF (Olafsson et al., 1995). It was therefore natural to test whether the GDNF effects are mediated by frequenin at these synapses. We first examined whether GDNF enhanced frequenin expression in vivo by injecting GDNF mRNA into the fertilized *Xenopus* eggs. Overexpression of GDNF significantly

increased the level of frequenin in 1-day-old (Figure 4A) and 2-day-old (data not shown) embryos, as detected by Western blot using an antibody specific for *Xenopus* frequenin. The expression of a neural-specific protein, Xefiltin (a *Xenopus* intermediate filament protein [Zhao and Szaro, 1997]) (Figure 4A, top), as well as other control proteins, such as actin and peripherin (Gervasi et al., 2000) (data not shown), remained constant. The frequenin signals were normalized to those of Xefiltin in the same blots, and the data from multiple experiments were averaged. The levels of frequenin in GDNF mRNA-injected embryos were ~2-fold of those in the control embryos (Figure 4A, bottom). In contrast, injection of mRNAs for NT3 or NT4, two neurotrophins also known to elicit long-term regulatory effects at these synapses (Wang et al., 1995; Wang and Poo, 1997), did not affect frequenin expression (Figure 4A, bottom).

Since the GDNF effects were observed at the NMJ, it is important to determine whether GDNF enhances frequenin expression in motoneurons. However, it was difficult to detect frequenin in the nerve-muscle cultures using Western blot, because there were only limited numbers of neurons in a single culture dish. We therefore used an alternative approach. Dorsal posterior parts (see Figure 4B, top) of 1-day-old *Xenopus* embryos injected with or without GDNF mRNA were dissected for
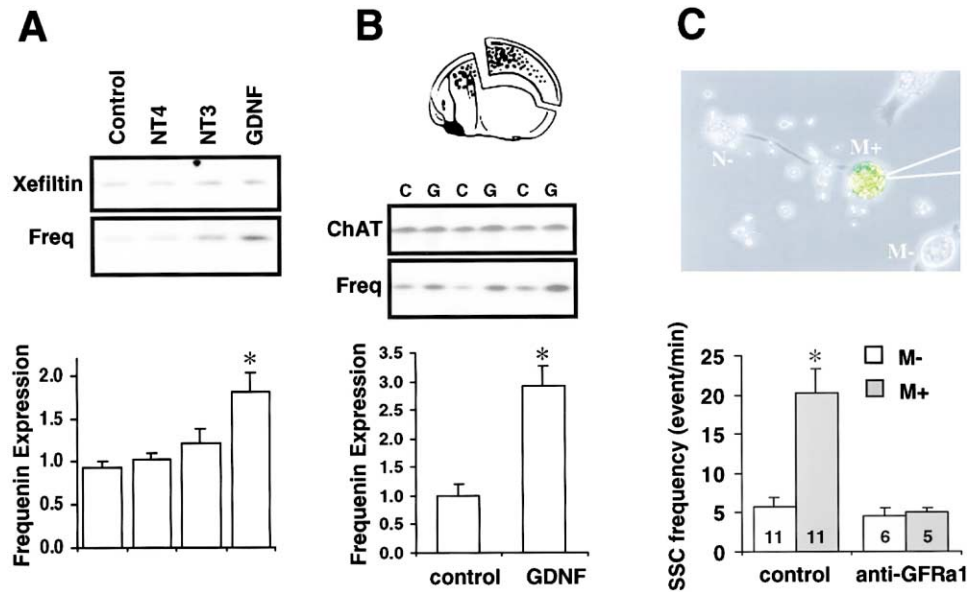
Figure 4. Effects of GDNF Overexpression in *Xenopus* Embryos

(A) Upregulation of frequenin expression in *Xenopus* embryos. GDNF, NT3, or NT4 mRNA was injected into *Xenopus* eggs, and the 1-day-old embryos were harvested at stage 40 for Western blot analysis. (Top) Examples showing the expression of frequenin (Freq, 24 kd) and the neurofilament protein Xefiltin (65 kd) in stage 40 1-day-old embryos. (Bottom) Summary of the effect of various neurotrophic factors on frequenin expression. The intensities of frequenin bands were normalized to those of Xefiltin bands in the same lanes, and the data from experiments using three independent batches of embryos were averaged. Note that frequenin levels were increased in embryos injected with GDNF mRNA but not NT3 or NT4 mRNA. *: $p < 0.05$, ANOVA test. (B) Upregulation of frequenin expression in spinal motoneurons. (Top) A schematic diagram showing the dissection of dorsal part of the embryos injected with or without GDNF mRNA. (Middle) Examples of frequenin and ChAT blots. C: Control. G: GDNF mRNA injected. (Bottom) Quantitation of Western blots based on five independent tissue samples. The frequenin signals were normalized to those of the motoneuron marker ChAT in the same blots. (C) Release of GDNF at the neuromuscular synapses. (Top) Superimposed phase and fluorescence images of nerve-muscle cocultures derived from GDNF mRNA-injected embryos. The postsynaptic myocyte expressing exogenous GDNF is indicated by GFP fluorescence. (Bottom) Effects of targeted expression of GDNF on SSC frequency. The cultures were in the presence of an antibody against the GDNF receptor GFR-α1 (50 ng/ml) for 1 day. Synapses with or without GDNF expressed in the postsynaptic myocytes (M+ and M− synapses) were recorded. Note that GDNF secreted from the postsynaptic cells enhances synaptic transmission, and anti-GFR-α1 blocks this effect.

Western blot. This tissue contains frequenin-expressing spinal cord (neural tube without brain) and myotomal tissues that do not express frequenin (Olafsson et al., 1995). At this stage of development, the majority of neurons derived from the spinal cord are ACh-secreting motoneurons (Xie and Poo, 1986). Moreover, we normalized the frequenin signals to those of the motoneuron marker choline acetyltransferase (ChAT) in the same blots. Dorsal tissues derived from control and GDNF mRNA-injected embryos exhibited very similar levels of ChAT (Figure 4B), suggesting that GDNF does not change the number of motoneurons in the spinal cords. Injection of GDNF mRNA significantly increased frequenin expression. On average, the levels of frequenin protein in the injected spinal cords were ∼300% of that in controls (Figure 4B, bottom). These results suggest that GDNF enhances the expression of frequenin in motoneurons.

Another important issue was whether overexpressed GDNF protein was released at the neuromuscular synapses. To address this issue, we injected GDNF mRNA together with mRNA for green fluorescence protein (GFP) into one of the blastomeres of two-cell stage embryos. Nerve-muscle cultures prepared from the injected embryos contained fluorescence-negative and -positive neurons and muscles (Figure 4C, top). GFP fluorescence has been shown to serve as an excellent indicator of

cells expressing the coinjected mRNA (Wang and Poo, 1997). We selected synapses in which exogenous GDNF was highly expressed in the postsynaptic muscle cells but not in presynaptic neurons, as indicated by the green fluorescence (N−/M+ synapses). Consistent with the effects of long-term bath application of GDNF, overexpression of GDNF in the postsynaptic muscle cells also markedly enhanced synaptic transmission. SSC frequency in N−/M+ synapses was five times that of N−/M− synapses (Figure 4C, bottom). Moreover, when cultures were incubated with an antibody (50 ng/ml) against GDNF receptor GFR-α1, the effect of postsynaptic GDNF expression was completely blocked (Figure 4C, bottom). These results strongly suggest that exogenous GDNF protein introduced into the developing *Xenopus* by embryo mRNA injection is released at the neuromuscular synapses, perhaps from the postsynaptic muscle cells, and that the released GDNF can be neutralized by the anti-GFR-α1 antibody.

GDNF Effects Are Attenuated by Frequenin Antisense Oligonucleotides/Antibody

If frequenin is downstream of GDNF modulation, inhibition of frequenin expression by antisense oligonucleotides (oligos) should attenuate the GDNF effects. We tested the ability of the oligos to inhibit frequenin expression in *Xenopus* embryos rather than in the nerve-mus-
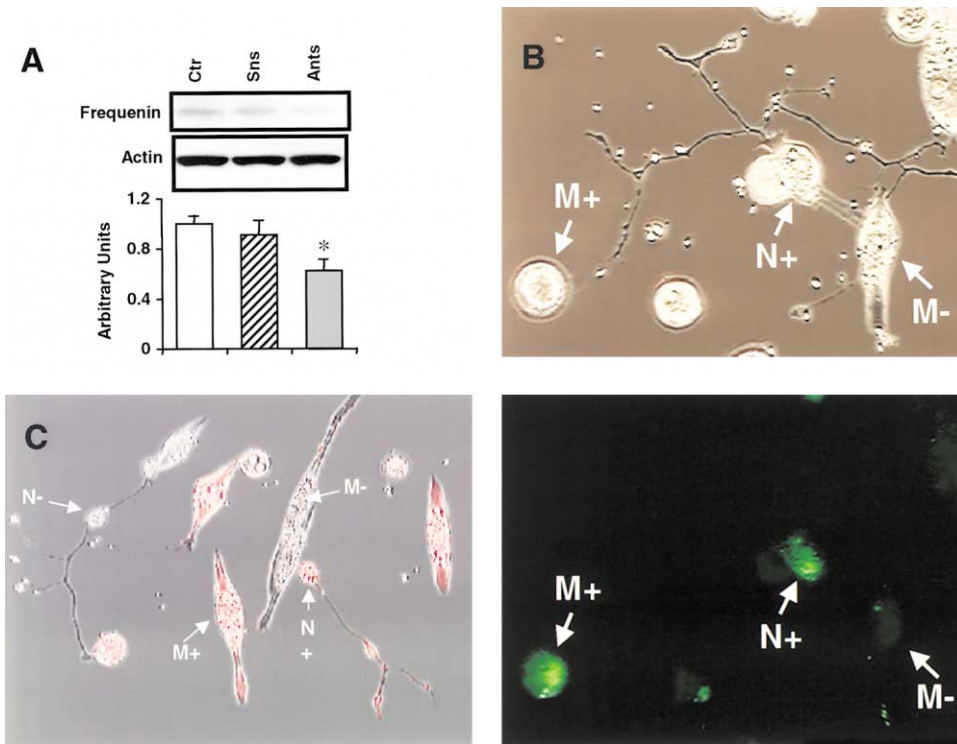
Figure 5. Strategies to Inhibit Frequenin Expression or Activity

(A) Inhibition of frequenin expression by frequenin antisense oligonucleotides (oligos). (Top) An example of the Western blots showing that the reduction of frequenin protein in stage 40 embryos injected with antisense (Ants) but not with sense (Sns) oligonucleotides at one-cell stage. Ctr: uninjected control. Actin was used as loading control. (Bottom) Quantitation of eight independent Western blots. (B) Phase (top) and fluorescence (bottom) images of cells transfected with (+) or without (−) oligos. GDNF was added to all cultures 6 hr after plating. Fluorescein-labeled antisense oligos were introduced to cultured cells by liposome-mediated transfection. (C) Superimposed phase and fluorescence images of cells loaded with (+) or without (−) anti-frequenin antibody. The antibody-containing cells were marked by coinjection of 70 kd rhodamine-dextran (red).

cle cultures because of the limited number of cells available in these cultures. Injection of antisense oligos but not sense oligos into *Xenopus* embryos reduced the levels of frequenin protein by half (Figure 5A). Other proteins, such as the cytoskeleton protein actin (Figure 5A) and α-tubulin and neurofilament protein (data not shown), were not affected. The 1-day-old nerve muscle cultures were transfected with antisense or sense oligos covalently labeled by fluorescein using a lipofectin method (Boehringer), followed by an extensive wash, and then treatment with GDNF for an additional 24 hr. Successful transfection was demonstrated by the presence of green fluorescent oligos inside neurons and myocytes (N+ and M+), while untransfected cells were nonfluorescent (N− and M−) (Figure 5B). We first tested whether antisense oligos affect basal synaptic transmission in the absence of GDNF. As shown in Figures 6A and 6B, SSC frequency, ESC amplitude, and synaptic delay recorded from synapses made by neurons transfected with antisense oligos (N+) and those made by untransfected (N−) neurons were essentially the same. Treatment with GDNF elicited potentiation of N− synapses, and these results were set as 100% (Figures 6D–6F). In contrast, GDNF had little effect on N+ synapses in the same culture. The N+ synapses exhibited a much-reduced SSC frequency and ESC amplitude compared with the N− synapses (Figures 6D and 6E). The synaptic delay in N+ synapses was also prolonged

(Figure 6F). Sense-frequenin did not block GDNF function (Figures 6D–6F). These effects were specific for presynaptic neurons because antisense-frequenin transfected into the postsynaptic muscle cells (M+) did not prevent the GDNF effects on the neuromuscular synapses (data not shown). Further, transfection of frequenin antisense oligos into neurons treated with NT3, which is known to enhance synaptic transmission in these cultures (Wang et al., 1995), did not attenuate the effect of NT3 (Figure 6C). Thus, frequenin antisense oligos selectively attenuate GDNF-induced synaptic potentiation rather than nonspecifically disrupt synaptic transmission.

As a complementary approach, we determined whether the GDNF effects could be neutralized by an affinity-purified antibody against frequenin (Olafsson et al., 1995). The antibody, together with rhodamine-dextran, was injected into *Xenopus* embryos at two-cell stage, and stage 22 embryos were used to prepare the nerve-muscle cocultures. Injection of anti-frequenin antibody did not affect the morphology or the development of the *Xenopus* embryos (data not shown), and the neurons and muscle cells appeared completely normal in these cultures (Figure 5C). We also compared the distribution of cells with fluorescein-conjugated control antibodies (IgG, green fluorescence) and that of cells with rhodamine-dextran (red fluorescence). Similar to previous reports (Alder et al., 1992), we found that the green
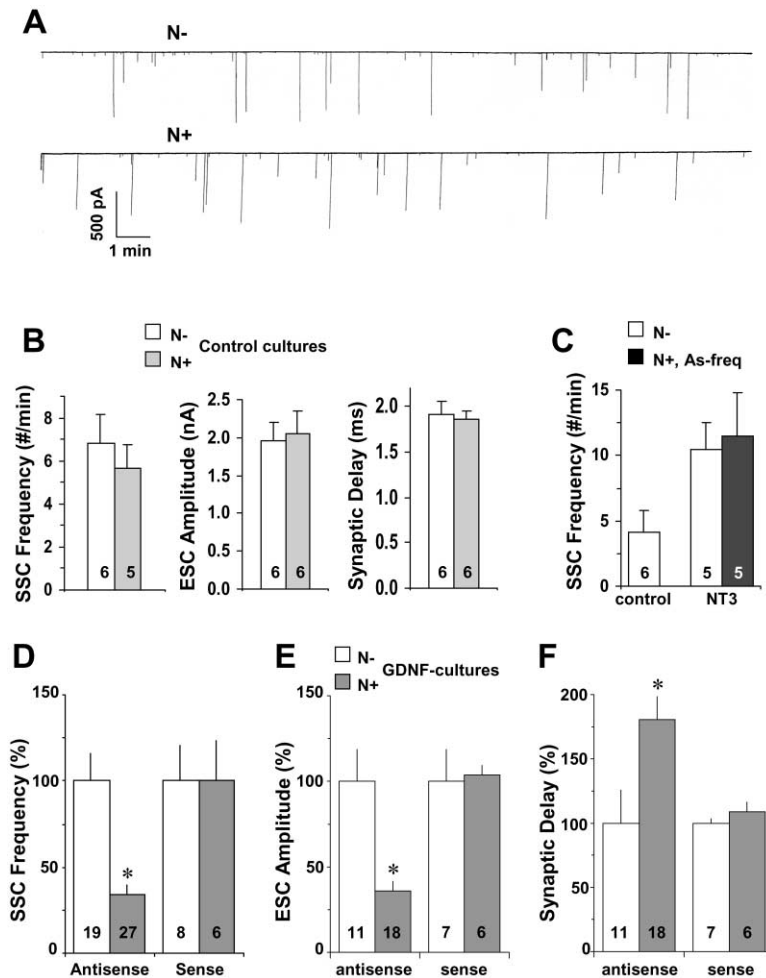
Figure 6. Blockade of Synaptic Effects of GDNF by Transfection of Frequenin Antisense Oligonucleotides

Transfected and untransfected motoneurons were identified by the presence (N+) or absence (N−) of green fluorescence, as indicated in Figure 5B. (A) Examples of SSCs recorded from an oligo-negative synapse (N−) or an oligo-positive synapse (N+). (B) Lack of effect of oligos on basal synaptic transmission in the absence of GDNF. Control cultures were transfected with antisense oligos. SSC frequency, ESC amplitude, and synaptic delay were measured in synapses made by transfected (N+) and untransfected (N−) motoneurons. (C) Frequenin antisense oligos do not affect NT3-induced synaptic facilitation. SSC frequency was measured in control and NT3-treated cultures. N+, As-freq: synapses made by neurons transfected with the oligo. (D–F) Effect of the antisense and sense oligos on SSC frequency (D), ESC amplitude (E), and synaptic delay (F) in GDNF-treated cultures. Results obtained from synapses made by untransfected neurons (containing no antisense, N−) were set as 100%.

and red fluorescence coexisted in more than 90% of cells (data not shown), suggesting that rhodamine-dextran fluorescence faithfully reflects the cells containing the coinjected antibody. Whole-cell recording indicated that basal synaptic transmission was not affected by the anti-frequenin antibody (Figure 7A). In contrast, the antibody significantly interfered with GDNF-induced synaptic potentiation. In synapses made by neurons not containing the antibody (N− synapses), GDNF markedly enhanced transmission, and these results were set as 100% (Figures 7B–7D). Introduction of anti-frequenin antibody but not a control antibody (rabbit IgG) to the presynaptic neurons (N+) reversed the GDNF effects on SSC frequency and ESC amplitude (Figures 7B and 7C) but not on synaptic delay (Figure 7D). It is unclear why the antibody decreased rather than increased synaptic delay in GDNF-treated cultures. One possibility is that frequenin uses different domains to interact with multiple targets. Anti-frequenin antibody may block only one (or few) of the functional domains, resulting in perplexing effects. Nevertheless, most of our antibody data provided additional support for the antisense oligo results.

GDNF Facilitates Ca²⁺ Influx at Motor Nerve Terminals
How does GDNF/frequenin potentiate presynaptic transmitter release? Classic experiments suggest that synap-

tic delay reflects the time for coupling of depolarization/Ca^{2+} influx to transmitter release (Llinas, 1982). The decrease in synaptic delay implies a modulation of Ca^{2+} influx by GDNF and frequenin, leading to more efficient vesicle fusion. We therefore examined the changes in intracellular Ca^{2+} ($[Ca^{2+}]_i$) by confocal microscopy using the cell-permeable, low-affinity Ca^{2+} indicator Oregon green 488 BAPTA-5N, AM (OG488, kd = 32 μM). The high Ca^{2+} on and off rates of the indicator allow rapid kinetic tracking of Ca^{2+} changes (Zhao et al., 1996). We measured the OG488 fluorescence within nerve terminals (varicosities) (Figure 8A) and normalized it to averaged basal fluorescence. The percentage of change in fluorescence ($\Delta F/F_{0\%}$) was plotted against time. Stimulation by a single pulse current injection evoked a rapid increase but slow decay of $[Ca^{2+}]_i$ (Figure 8B and Supplemental Movie S1), typically seen at the nerve terminals of these motoneurons and other CNS neurons (Koester and Sakmann, 2000; Ming et al., 2001). The amplitude of $[Ca^{2+}]_i$ responses was significantly higher in GDNF-treated terminals compared with that in untreated controls (Figure 8B). To elucidate the mechanisms for GDNF-induced modulation of synaptic delay, which is in the range of 1–2 ms in these neurons (Figure 2), we measured terminal $[Ca^{2+}]_i$ transient with very high temporal resolution (480 frames/s). Within 2 ms after electric stimulation of the neuronal soma, the shortest time win-
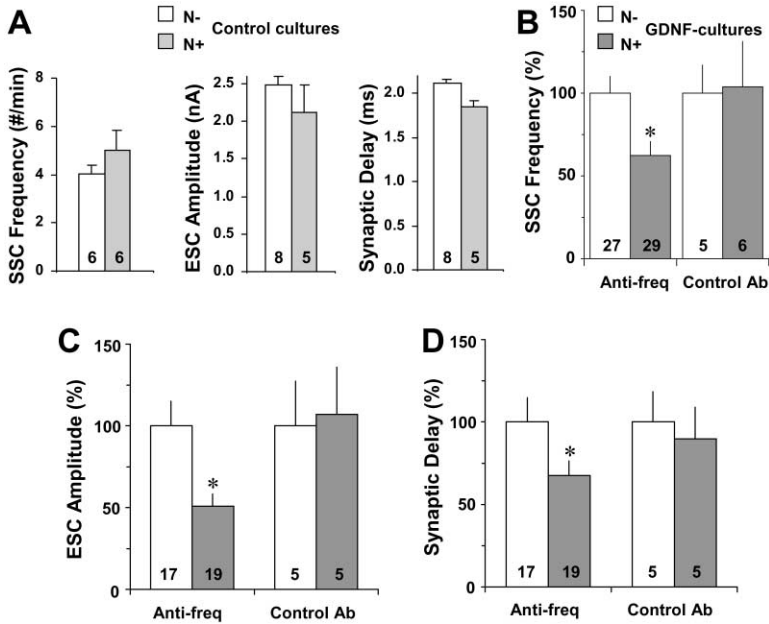
Figure 7. Blockade of Synaptic Effects of GDNF by Anti-Frequenin Antibody

The antibody was introduced into motoneurons by embryo injection techniques. Antibody-containing motoneurons were identified by the presence (N+) or absence (N−) of red fluorescence, as indicated in Figure 5C. (A) Lack of effect of the anti-frequenin antibody on basal synaptic transmission in the absence of GDNF. SSC frequency, ESC amplitude, and synaptic delay were measured in N− and N+ synapses. (B–D) Effect of the anti-frequenin (Anti-freq) or IgG control (control Ab) antibodies on SSC frequency (B), ESC amplitude (C), and synaptic delay (D) in GDNF-treated cultures. Results obtained from N− synapses were set as 100%.

dow that we could measure, we observed a large increase in OG488 fluorescence (expressed as F/F_0) in both control and GDNF-treated terminals (Figure 8C), suggesting an increase in $[Ca^{2+}]_i$ within such a time window. Neurons treated with GDNF exhibited a 2-fold increase in terminal $[Ca^{2+}]_i$ after electrical stimulation, as compared to control neurons (Figure 8C). It is conceivable that enhancement of Ca^{2+} influx by GDNF treatment results in a decrease in synaptic delay and an increase in amplitude of ESCs.

GDNF/Frequenin Potentiates Ca²⁺ Channels

An enhancement of Ca^{2+} influx could be due to an increase in action potential duration of presynaptic moto-

neurons. However, we found that long-term treatment with GDNF did not significantly alter the action potential duration in *Xenopus* motoneurons (Figure 9A). Alternatively, direct modulation of Ca^{2+} channels could lead to an enhanced Ca^{2+} influx. We recorded the Ca^{2+} currents under the whole-cell, voltage-clamped configuration from spinal neurons grown in the presence or absence of GDNF for 1 day. Ca^{2+} currents were isolated by blocking Na^+ currents with external TTX (1 μM) and K^+ currents with external tetraethylammonium (TEA, 115 mM) and internal Cs^+ (90 mM). The remaining currents were completely blockable by 0.5 mM Cd^{2+}, suggesting that they are Ca^{2+} currents (data not shown). By subtracting currents elicited by two depolarization proto-
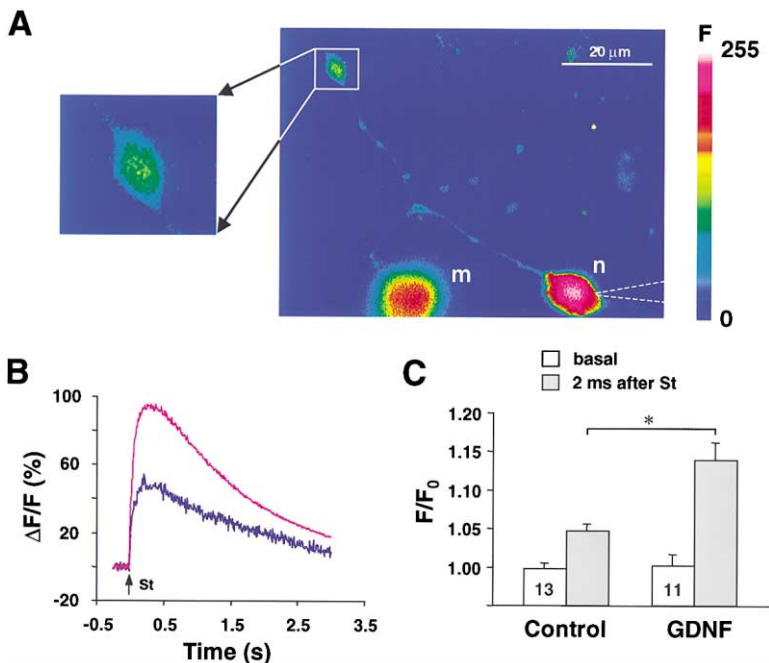

Figure 8. Effect of GDNF on Ca²⁺ Influx

Neuronal varicosities (terminals) were imaged in a confocal microscope using OG488 as an indicator. (A) An example of images from GDNF-treated neurons filled with the indicator. The image of a varicosity is enlarged and presented on the left. The pseudocolor scale shows approximate fluorescence intensity values in 8 bit scale. n, neuron; m, muscle. Dotted lines indicate the position of a stimulation electrode. (B) Example traces showing fluorescence intensity plotted against time. Fluorescence intensity was measured and normalized using the $\Delta F/F_0$ procedure. St, time point neurons were stimulated. (C) Summary of Ca^{2+} transients before and 2 ms after electrical stimulation. The data were normalized to initial value F_0 and expressed as F/F_0.
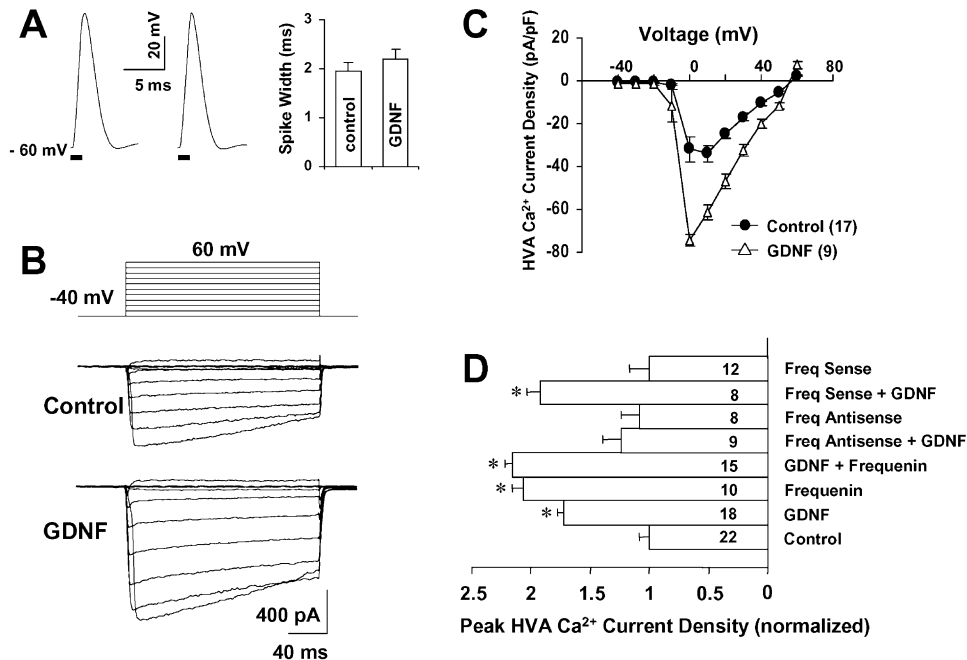
Figure 9. Effect of GDNF and Frequenin on Ionic Properties of Motoneurons

(A) GDNF has no effect on action potential duration. A suprathreshold 1 ms (indicated by the black bar) depolarizing current was injected into the motoneurons under current-clamp conditions to induce action potentials. Spike half-width was measured with the membrane potential held at −60mV. No differences were observed in resting membrane potential, input resistance, or spike amplitude between control and GDNF-treated motoneurons (data not shown). n = 10 for control; n = 9 for GDNF-treated neurons. (B) Example of HVA Ca^{2+} currents from control and GDNF-treated spinal neurons. Ca^{2+} currents were isolated from other currents in the motoneurons treated with or without GDNF for 1 day and recorded under the whole-cell, voltage-clamped conditions. Depolarizing current steps were applied at 10mV increments from −40mV to +60mV, starting from a holding voltage of −40mV. (C) Peak current density-voltage relations (I-V curves) for HVA Ca^{2+} current density recorded from control and GDNF-treated spinal neurons. (D) GDNF modulation of HVA Ca^{2+} currents is mediated by frequenin. The nerve-muscle cultures, either derived from frequenin protein-injected embryos or transfected with frequenin antisense or sense oligos, were treated with or without GDNF for 1 day. I-V curves under different experimental conditions were constructed and the peak current densities at 0mV presented.

cols (one −90mV to +60mV, the other −40mV to +60mV, both with 10mV increments), we observed two Ca^{2+} current components: a small transient inward current activated by small depolarizing step (putative T currents) and a large sustained inward current activated only when the depolarization step was higher than −10mV (high-voltage activated or HVA currents). As shown in Figure 9B, a series of 200 ms step depolarization, from −40mV to +60mV in 10mV increments (holding potential −40mV) elicited typical HVA inward Ca^{2+} currents of variable sizes. Treatment with GDNF had no effect on T currents (data not shown). In contrast, GDNF markedly increased the amplitude of HVA Ca^{2+} currents. To correct for variability of neuronal sizes, peak current density (peak current/capacitance) of each neuron was calculated, and the averaged number was used to construct current-voltage relations (I-V curves). Compared with control neurons, GDNF pretreatment increased the Ca^{2+} current density by ∼120% when measured at 0mV (Figure 9C).

To investigate whether GDNF-induced potentiation of Ca^{2+} currents was mediated by frequenin, we measured HVA currents in neurons loaded with frequenin protein by embryo injection or in those transfected with frequenin antisense oligos. Peak Ca^{2+} current densities of cells at 0mV under different experimental conditions are sum-

marized in Figure 9D. The current densities in neurons treated with GDNF were significantly higher than those in control neurons. Introduction of exogenous frequenin protein into the spinal neurons (through embryo injection) also elicited a marked increase in Ca^{2+} current density (Figure 9D). The effect of GDNF was attenuated in neurons transfected with antisense- but not sense-frequenin oligos (Figure 9D). Treatment with antisense oligos alone had no effect on the current density (Figure 9D), possibly because the level of endogenous frequenin is very low at this stage of development (Olafsson et al., 1995). Furthermore, the increased Ca^{2+} current density elicited by expressing exogenous frequenin occluded that induced by GDNF (Figure 9D). These results suggest that GDNF-induced potentiation of Ca^{2+} channels is mediated by frequenin.

GDNF Promotes N-type Ca^{2+} Channel Activation
We next determined specific type(s) of channels regulated by GDNF. In control cultures, application of the L-type channel blocker nifedipine (20 μM) and the N-type channel blocker ω-conotoxin GVIA (10 μM) together virtually abolished all Ca^{2+} currents (data not shown), suggesting that L- and N-types of channels are the major Ca^{2+} channels in the cell bodies of these spinal neurons. When L-type channels were blocked by nifedi-
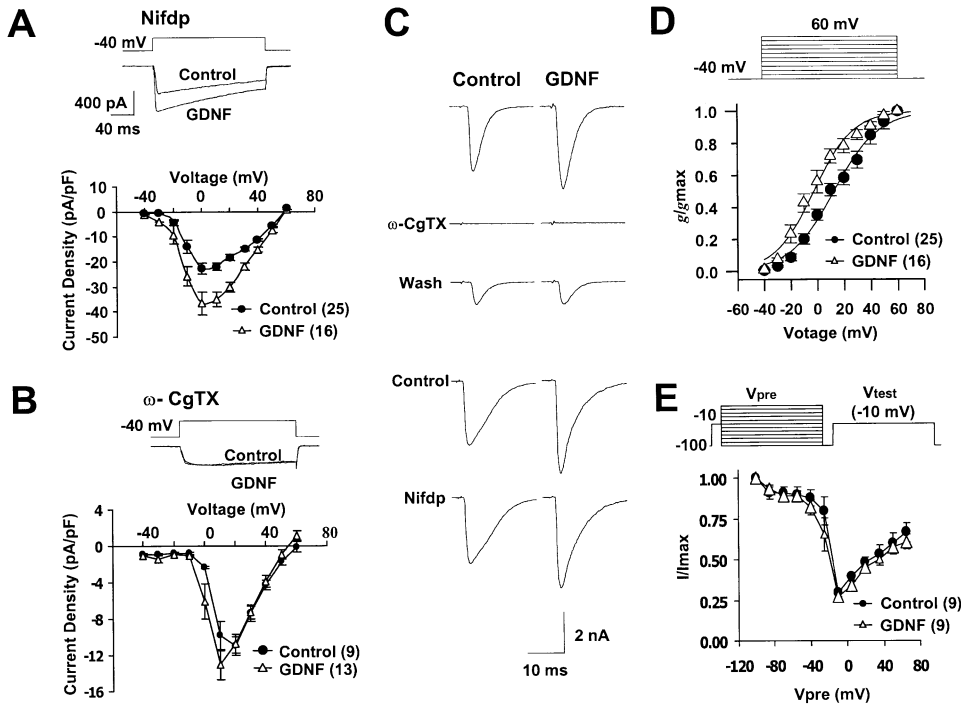
Figure 10. GDNF Regulation of the Properties of N- but Not L-type Ca^{2+} Channels

(A and B) *Xenopus* spinal neurons were grown in the presence or absence of GDNF for 1 day, treated with either the L-type channel blocker nifedipine (Nifdp) or the N-type channel blocker ω-conotoxin GVIA (ω-CgTX) for 30 min before recording of Ca^{2+} currents. Examples of current traces are shown above the I-V curves. Note that GDNF still elicits a 2-fold increase in Ca^{2+} currents (A) in Nifdp-treated neurons but has no effect on ω-CgTX-treated neurons (B). (C) Role of N- and L-type Ca^{2+} channels in evoked synaptic transmission. (Top) In both control and GDNF-treated synapses, perfusion of the ω-CgTX completely blocked evoked transmission. Perfusion of Ringer solution for 5 min (Wash) partially reverses the effect of ω-CgTX. (Bottom) Perfusion of Nifdp has no effect on ESCs. (D and E) Steady-state activation and inactivation curves. Nifedipine, in addition to all other channel blockers, was used in all recordings. (D) Activation curves. N-type Ca^{2+} currents were generated by a series of test depolarization shown on top (V_{test}). The reversal membrane potential (V_{rev}) under our recording conditions was −58mV. Membrane conductance (g) at different test potentials were obtained by dividing the peak current density by the current driving force (V_{test}-V_{rev}), and were normalized to that collected at +60mV depolarization (gmax). The data were fitted with a Boltzmann function: $g/gmax = 1/\{1 + exp[-(V - V_{1/2})/k]\}$, where V is the membrane potential, $V_{1/2}$ is the membrane voltage at which the current amplitude is half-maximum, and k is the slope factor. (E) Inactivation curves. A two-pulse depolarization protocol is shown on top. A 100 ms depolarization prepulse to various voltages (V_{pre}) was applied to the motoneuron, followed by a second depolarization test pulse (V_{test}). The peak currents elicited by V_{test} were plotted against the different V_{pre} steps.

pine, total Ca^{2+} currents were slightly reduced (compare Figures 9C and 10A). GDNF still elicited a marked increase in the N-type Ca^{2+} currents (Figure 10A). In contrast, when N-type channels were blocked by ω-conotoxin GVIA, GDNF no longer affect HVA Ca^{2+} currents (Figure 10B). These results strongly suggest that GDNF potentiates N-type but not L-type Ca^{2+} channels. The N-type Ca^{2+} channels are known to be involved in coupling Ca^{2+} influx and transmitter release in the *Xenopus* motoneurons (Yazejian et al., 1997). Perfusion of ω-conotoxin GVIA completely and reversibly blocked evoked release, whereas that of nifedipine had little effect on ESCs (Figure 10C), suggesting that N-type is the major Ca^{2+} channel at the nerve terminals. Thus, modulation of N-type Ca^{2+} channels contributes directly to GDNF/frequenin-induced potentiation of synaptic transmission.

To understand how GDNF modulates N-type Ca^{2+} channels, we examined the effect of GDNF on N-type channel kinetics. We constructed steady-state activation curves based on the current-voltage relationships shown in Figure 10A. Treatment with GDNF produced a 10.3mV leftward shift in the activation curve (Figure 10D). The membrane voltage at which the current amplitude is half-maximum, or $V_{1/2}$, was 12.7mV ± 2.4mV for control and 2.4mV ± 2.1mV for GDNF-treated cells, respectively (p < 0.01). Thus, at any given depolarization voltage, GDNF increases the opening probability of N-type Ca^{2+} channels. The steady-state inactivation curves were constructed by a two-pulse depolarization protocol (Figure 10E) (Jones et al., 1999). A 100 ms depolarization pulse to various voltages (V_{pre}, from −100mV to +65mV, 15mV increments) was applied to the motoneuron to inactivate N-type channels to different extents. Following a brief pulse (10 ms), a second depolarization pulse (V_{test}, 100 ms, −10mV) was applied to determine the proportion of Ca^{2+} channels available for activation. The peak currents elicited by V_{test} were plotted against the different V_{pre} steps (Figure 10E). The inactivation curves derived from control and GDNF-treated cells looked almost identical (Figure 10E). Therefore, GDNF potentiates N-type Ca^{2+} channels by facilitating their steady-state activation without affecting their inactivation, although we do not know whether GDNF affects the number of functional channels.

Discussion

There are three main findings in the present study. First, we report a GDNF-induced long-term facilitation of neurotransmitter release at the neuromuscular synapses. Second, we show that the effect of GDNF on synaptic transmission is mediated by an increase in the expression of the Ca^{2+} binding protein frequenin. Finally, we demonstrate that GDNF and frequenin facilitate synaptic transmission by enhancing N-type Ca^{2+} channel activation, leading to an enhancement of Ca^{2+} influx. Thus, this study has identified a molecular target that mediates the long-term, synaptic action of a neurotrophic factor. Our findings may also provide important insights into the regulatory mechanisms of neurotransmitter release.

In contrast to the rapid progress in understanding the acute modulation of synapses by neurotrophins, studies on long-term neurotrophic regulation of synaptic transmission have been very limited. However, high level of expression and largely constitutive secretion of neurotrophic factors in the nervous system suggest that long-term regulation of synaptic transmission and plasticity may be just as an important and perhaps more common form of neurotrophic regulation. We report here that GDNF markedly enhances transmitter release at the NMJ. GDNF has recently been reported to increase the number of nerve terminals at the NMJ in vivo (Nguyen et al., 1998) and to enhance transmitter release in midbrain dopaminergic neurons in culture (Bourque and Trudeau, 2000). Our present study, together with the previous studies on GDNF and neurotrophins, suggest that long-term modulation of synaptic strength by neurotrophic factors is a general and physiologically relevant phenomenon.

GDNF/frequenin-induced enhancement of transmitter release could be due to an increase either in the probability of transmitter release (Pr) or in the number of release sites (N). Several pieces of evidence suggest that the increase in Pr is responsible for most of the increase in transmitter release. First, GDNF decreased PPF, a short-term plasticity frequently used to monitor changes in Pr (Zucker, 1989). Second, direct measurement of transmitter release using FM dye indicated that the rate of FM dye destaining was significantly faster at presynaptic boutons treated with GDNF, as compared with that in control boutons. The decrease in the time constant τ by GDNF was more effective at lower $[Ca^{2+}]_o$, while the total amount of destaining in normal $[Ca^{2+}]_o$ (ΔF) was not significantly affected. Since changes in τ reflect changes in Pr, particularly at lower $[Ca^{2+}]_o$, these results strongly suggest that GDNF increases Pr. Third, GDNF/frequenin decreased synaptic delay, an electrophysiological parameter that measures mainly the excitation-secretion coupling. Finally, GDNF markedly increases Ca^{2+} influx into the presynaptic terminals. Changes in Ca^{2+} influx directly affects Pr. While these experiments support the view that GDNF increases Pr, we could not rule out the possibility that an increase in N also contributes to GDNF-induced enhancement of transmitter release. The fact that GDNF-induced increase in SSC frequency (4- to 5-fold) was more pronounced than that in ESC amplitude (2-fold) implies changes in N in addition to Pr. Although we do not have direct evidence that GDNF facilitates the formation of new release sites at the NMJ, we found that the number as well as the size of synaptic varicosities (as measured by synaptobrevin-GFP fluorescent spots) was increased in cultures treated with GDNF (B.L. and H.-S. Je, unpublished data).

An important finding in the present study is that GDNF facilitates evoked transmitter release by enhancing Ca^{2+} influx through N-type Ca^{2+} channels. A reduction of synaptic delay reflects facilitation of excitation-secretion coupling most likely explained by an enhancement of Ca^{2+} influx within the millisecond time window after stimulation. We found that neurons treated with GDNF exhibited almost twice as much increase in $[Ca^{2+}]_i$ within 2 ms after a brief ($\sim$1 ms) electrical stimulation. Such a rapid increase in $[Ca^{2+}]_i$ will undoubtedly facilitate transmitter release, leading to an increase in ESC amplitude and a reduction in synaptic delay. The relatively slow decay (half decay time $\sim$1.5 s) in $[Ca^{2+}]_i$ transient induced by a single action potential is typical of these developing neurons, and a similar time course of Ca^{2+} influx was observed by other investigators (Koester and Sakmann, 2000; Ming et al., 2001). It is possible that the mechanisms for removing excess free Ca^{2+}, such as Ca^{2+} uptake into mitochondria or Ca^{2+} pumps and/or exchangers, are not well developed in these motoneurons. GDNF does not appear to alter the kinetics of $[Ca^{2+}]_i$ decay. GDNF potentiates Ca^{2+} influx by facilitating the activation but not the inactivation of N-type Ca^{2+} channels. Since the N-type channels are the major Ca^{2+} channel type at the terminals of these motoneurons, potentiation of this channel by GDNF/frequenin will undoubtedly result in an increase in Ca^{2+} influx during evoked transmission.

The present study indicates that GDNF enhances presynaptic transmitter release through upregulation of frequenin. These findings have two important implications. First, we have identified a molecular target that mediates the synaptic action of a neurotrophic factor. A general problem in the field has been the difficulty in determining specific downstream molecules responsible for the synaptotrophic actions of any factors because they are usually involved in multiple functions in the nervous system. We now provide evidence that (1) GDNF enhances frequenin expression in motoneurons; (2) GDNF and frequenin have almost identical long-term effects on synaptic transmission and Ca^{2+} channels at NMJ; and (3) inhibition of frequenin function by two independent approaches attenuated the effects of GDNF. These results qualify frequenin as one of the downstream targets that mediates GDNF-induced enhancement of synaptic transmission at NMJ. Second, this work may provide important insights into mechanisms by which synaptic transmission is modulated. We showed that GDNF enhances transmitter release at NMJ through frequenin, a cytosolic protein that binds Ca^{2+} with high affinity (Pongs et al., 1993; Olafsson et al., 1995). We also demonstrated that GDNF/frequenin enhances Ca^{2+} influx during evoked transmission by potentiating N-type Ca^{2+} channel activity. Recently, null mutation of frequenin in *C. elegans* has been shown to impair associative learning and memory (Gomez et al., 2001). Since frequenin is expressed in neurons throughout the brain (Paterlini et al., 2000), it is tempting to speculate that it may serve as a general modulator for Ca^{2+}-depen-

dent synaptic transmission and plasticity in the nervous system.

Exactly how frequenin acts to potentiate transmitter release is an interesting question that requires further investigation. Since the affinity of frequenin to Ca^{2+} is relatively high (<1 μM) and the levels of frequenin in the nervous system is relatively low, the primary role of frequenin is not to buffer cellular Ca^{2+} during evoked transmission (Pongs et al., 1993; Olafsson et al., 1995). One possibility is that frequenin activates PI4K (Hendricks et al., 1999), a protein localized in synaptic vesicles and implicated in transmitter release (Wiedemann et al., 1998). Alternatively, frequenin may directly interact with N-type Ca^{2+} channels. The Ca^{2+} binding protein calmodulin has been demonstrated to modulate L-type and P/Q-type Ca^{2+} channels by direct binding to the C-terminal sequences of the Ca^{2+} channels (Lee et al., 1999; Peterson et al., 1999; Zuhlke et al., 1999). Proteins that interact with N-type Ca^{2+} channels have yet to be identified. Since frequenin is a Ca^{2+} binding protein with the overall structure similar to that of calmodulin (Olafsson et al., 1995), it will be interesting to determine whether frequenin interacts directly with N-type Ca^{2+} channel to regulate its activity.

Experimental Procedures

Culture Preparation
Neural tube and associated myotomal tissue of stage 20 *Xenopus* embryos were dissociated in Ca^{2+}- and Mg^{2+}-free medium (58.2 mM NaCl, 0.7 mM KCl, 0.3 mM EDTA [pH 7.4]). The cells were plated on glass coverslips and grown in the presence or absence of GDNF (40 pM) for 1 day at room temperature, as described (Wang et al., 1995). The culture medium consisted (vol/vol) of 50% L-15 medium, 1% fetal calf serum, and 49% Ringer's solution (117.6 mM NaCl, 2 mM CaCl2, 2.5 mM KCl, 10 mM HEPES [pH 7.6]). GDNF (40 pM) was added to the cultures 6 hr after plating, when cells were completely settled.

Electrophysiology
Synaptic currents were recorded from innervated muscle cells in 1-day-old cultures by whole-cell recording methods at room temperature (Wang et al., 1995). The solution inside the recording pipette contained (mM) KCl, 150; NaCl, 1; MgCl$_2$, 1; and HEPES buffer, 10 (pH 7.2). To elicit ESCs, square current pulses (0.5–1 ms, 0.5V–5V) were applied to neuronal soma under loose-seal conditions with a patch electrode filled with Ringer's solution. Data were collected and filtered at 3 kHz. SSC frequency is defined as the number of SSC events per minute. The amplitudes of SSCs and ESCs were analyzed using SCAN software (Dagan, Inc.). The waveform of SSCs for each synapse was generated by averaging the aligned peaks of at least 100 SSC events. The waveforms from multiple synapses were then averaged. Ca^{2+} currents were monitored as described (Jones et al., 1999). Culture medium was replaced with external solution containing (mM) CaCl$_2$, 6; HEPES, 10 (pH 7.6). TTX (1 μM) and tetraethylammonium (TEA, 115 mM) were included in the external solution to block Na^+ and K^+ channels, respectively. Pipette and membrane capacitance and serial resistance were compensated. The patch electrode was filled with (mM) CsCl, 90; MgCl$_2$, 5; Mg-ATP, 4; EGTA, 10; HEPES, 10 (pH 7.4). Ca^{2+} currents were evoked by 10mV, 200 ms depolarizing steps from -90mV for low-voltage activated currents (LVA) or -40mV for high-voltage activated currents (HVA). Data were collected using Clampex software with a current signal filter at 3 kHz and analyzed using Clampfit (pClamp 7 package, Axon Instruments).

FM1-43 Imaging
The FM dye experiments were carried out as previously described (Ryan et al., 1993), with minor modifications. In brief, FM1-43 (Molec-

ular Probes) was loaded into the spinal neurons by incubating 1-day-old cultures with high K^+ loading solution containing 2 μM FM1-43 and (mM) KCl, 60; NaCl, 57.6; CaCl$_2$, 3.5; HEPES, 10 (pH 7.6) for 3 min. Cells were rinsed ten times with wash solutions with different $[Ca^{2+}]_o$ (similar to Ringer's except $[Ca^{2+}]$ was adjusted to 0.1 mM, 0.5 mM, or 2 mM). Microscopy was conducted with a Noran Odyssey II confocal laser-scanning unit coupled to an upright microscope. Cells were illuminated with the 488 nm line Argon Ion laser at 10% of laser power (20 μW) delivered to the back aperture of a 40$\times$ water emersion lens (N.A. 0.80), with a band-pass excitation filter at 488 nm and a 515 nm long-pass emission filter. A 640 $\times$ 480 pixel image (0.23 μm/pixel) was obtained with the scan speed set at a dwell time of 3.2 μs such that images were acquired at a rate of 1 Hz. The fluorescence was stable with minimum bleach for more than 10 min in wash solutions. After acquiring 30 images (30 s) as baseline, FM1-43 destaining was initiated by rapid perfusion of high K^+ destaining solution that was essentially the same as the wash solution except that 117.6 mM NaCl was replaced by 60 mM of KCl and 57.6 mM of NaCl, and acquisition was continued for another 3 min at a rate of 1 Hz. The image data were stored in a SGI workstation and analyzed offline by Intervision 2D software (Noran). Fluorescence intensities were extracted from time-lapse images of individual boutons. The data were normalized to prede-staining fluorescence, fitted by single exponential curves, and time constants (τ) were obtained and averaged.

Embryo Injection
Recombinant frequenin or affinity-purified anti-frequenin antibody (Olafsson et al., 1995) was dialyzed against intracellular pipette solution and concentrated to 1 mg/ml. GDNF, NT3, or NT4 mRNAs (1 μg/μl) were mixed with GFP mRNA (1 μg/μl), and frequenin or anti-frequenin antibodies (1 μg/μl) were mixed with rhodamine-dextran (10 μg/μl, MW 40,000 or 70,000, respectively), all at 1:1 ratio. Approximately 6–12 nl of the solution was injected into one blastomere of embryos at the two- to four-cell stage. The final concentration of the protein or mRNA within an injected blastomere was $\sim$5 ng/μl. One day after injection, neural tubes and the associated myotomal tissues were dissected and used to prepare nerve-muscle cultures.

Ca^{2+} Imaging
The cultures were grown in the presence or absence of GDNF for 24 hr prior to examination by a Noran Odyssey II confocal microscope. Cells were excited using the 480 nm line of an Argon laser, and fluorescence was measured through a standard fluorescein filter set. To detect high-amplitude, fast Ca^{2+} transient, we used a cell-permeable, low-affinity Ca^{2+} indicator OG488 (kd = 32 μM). A stock solution of 5 mM was prepared using 20% w/v Pluronic in DMSO. The stock was diluted in Ringer's solution to a final concentration of 5 μM. Control and GDNF-treated cells were rinsed with Ringer's solution, loaded with OG488 for 5 min, followed by two rinses with Ringer's solutions. Neurons were stimulated at soma with a single-pulse current injection to induce an ESC. Stimulation was triggered during image acquisition such that the stimulus was synchronized with the image acquisition to preserve temporal resolution. A high rate of acquisition was achieved by reducing the image area, and single frames (160 $\times$ 120) were acquired at 480 frames per second. Fluorescence intensity (F) was measured using Intervision 2D software (Noran), with a region-of-interest tool outlining the nerve terminals (varicosities). The data were normalized to prestimulation fluorescence (F_0) post hoc and presented either as F/F_0 or $\Delta F/F_0$.

Transfection of Oligonucleotides
Frequenin oligonucleotides (antisense: 5'-CCTCCACCCACCTCAG GCTTCAG-3' and sense: 5'-CTGAAGCCTGAGGTGGTGGAGG-3') were labeled with fluorescein at the 5' ends and purified with HPLC. The first and last three nucleotides of the oligonucleotides were modified with phosphorothioates (S-oligo). First, *Xenopus* neurons and muscle cells were plated onto glass coverslips. Six hours later, the cells were transfected with the oligos (5 μg) for 3 hours, using the liposomal transfection reagent DOTAP (Boehringer) according to the manufacturer's instructions. Cells were washed three times and incubated with GDNF for another 24 hr before recording.

Western Blotting

Xenopus embryos (1- or 2-day-old) were homogenized in extraction buffer (100 mM NaCl, 50 mM Tris-HCl [pH 7.5], 1% NP-40, 2 mM PMSF, 1 μg/ml aprotinin, 1 μg/ml leupeptin, 1 μg/ml pepstatin A, 2 mM Na$_3$VO$_4$) and subsequently sonicated. Insoluble yolk proteins were discarded by centrifugation (12,000 × g, 20 min). The supernatants were transferred to a fresh tube containing 300 μl Freon (1,1,2-trichlorotrifluoroethane) (Sigma) vortexed for 1 min, incubated on ice for 5 min, and centrifuged again. The protein concentrations of the supernatants were determined using the BioRad protein assay. To determine frequenin expression in motoneurons, the dorsal parts of 1-day-old embryos (excluding brain) were quickly dissected. The tissues dissected from three embryos were pooled and proteins prepared the same way as above except that no Freon extraction was necessary. Equal amounts of proteins were loaded into SDS gels and blotted onto Immobilon-P membrane (Millipore). The blots were probed with an affinity-purified antibody against *Xenopus* frequenin (1:200; Olafsson et al., 1995), monoclonal antibodies against actin (1:1000; Chemicon) or choline acetyltransferase (ChAT, 1:100; Boehringer), or polyclonal antibodies against Xefiltin (1:300; Zhao and Szaro, 1997), *Xenopus* peripherin (1:300; Gervasi et al., 2000). The blots were then reacted with a secondary antibody conjugated with HRP, and specific signals were detected by chemiluminescence (Pierce).

References

Alder, J., Xie, Z.-P., Valtorta, F., Greengard, P., and Poo, M.-M. (1992). Antibodies to synaptophysin interfere with transmitter secretion at neuromuscular synapses. Neuron *9*, 759–768.

Baloh, R.H., Enomoto, H., Johnson, E.M., Jr., and Milbrandt, J. (2000). The GDNF family ligands and receptors—implications for neural development. Curr. Opin. Neurobiol. *10*, 103–110.

Boulanger, L., and Poo, M.M. (1999). Presynaptic depolarization facilitates neurotrophin-induced synaptic potentiation. Nat. Neurosci. *2*, 346–351.

Bourque, M.J., and Trudeau, L.E. (2000). GDNF enhances the synaptic efficacy of dopaminergic neurons in culture. Eur. J. Neurosci. *12*, 3172–3180.

Cabelli, R.J., Horn, A., and Shatz, C.J. (1995). Inhibition of ocular dominance column formation by infusion of NT-4/5 or BDNF. Science *267*, 1662–1666.

Chang, S., and Popov, S.V. (1999). Long-range signaling within growing neurites mediated by neurotrophin-3. Proc. Natl. Acad. Sci. USA *96*, 4095–4100.

Cohen-Cory, S., and Fraser, S.E. (1996). Effects of brain-derived neurotrophic factor on optic axon branching and remodelling in vivo. Nature *378*, 192–196.

Figurov, A., Pozzo-Miller, L., Olafsson, P., Wang, T., and Lu, B. (1996). Regulation of synaptic responses to high-frequency stimulation and LTP by neurotrophins in the hippocampus. Nature *381*, 706–709.

Gervasi, C., Stewart, C.B., and Szaro, B.G. (2000). Xenopus laevis peripherin (XIF3) is expressed in radial glia and proliferating neural epithelial cells as well as in neurons. J. Comp. Neurol. *423*, 512–531.

Gomez, M., De Castro, E., Guarin, E., Sasakura, H., Kuhara, A., Mori, I., Bartfai, T., Bargmann, C.I., and Nef, P. (2001). Ca(2+) signaling via the neuronal calcium sensor-1 regulates associative learning and memory in *C. elegans*. Neuron *30*, 241–248.

Gonzalez, M., Ruggiero, F.P., Chang, Q., Shi, Y.J., Rich, M.M., Kraner, S., and Balice-Gordon, R.J. (1999). Disruption of TrkB-mediated signaling induces disassembly of postsynaptic receptor clusters at neuromuscular junctions. Neuron *24*, 567–583.

Gottschalk, W., Pozzo-Miller, L.D., Figurov, A., and Lu, B. (1998). Presynaptic modulation of synaptic transmission and plasticity by brain-derived neurotrophic factor in the developing hippocampus. J. Neurosci. *18*, 6830–6839.

Gottschalk, W.A., Jiang, H., Tartaglia, N., Feng, L., Figurov, A., and Lu, B. (1999). Signaling mechanisms mediating BDNF modulation of synaptic plasticity in the hippocampus. Learn. Mem. *6*, 243–256.

He, X., Yang, F., Xie, Z., and Lu, B. (2000). Intracellular Ca^{2+} and Ca^{2+}/calmodulin-dependent kinase II mediate acute potentiation of neurotransmitter release by neurotrophin-3. J. Cell Biol. *149*, 783–792.

Henderson, C.E., Phillips, H.S., Pollock, R.A., Davies, A.M., Lemeulle, C., Armanini, M., Simmons, L., Moffet, B., Vandlen, R.A., Simpson, L.C., et al. (1994). GDNF: a potent survival factor for motoneurons present in peripheral nerve and muscle. Science *266*, 1062–1064.

Hendricks, K.B., Wang, B.Q., Schnieders, E.A., and Thorner, J. (1999). Yeast homologue of neuronal frequenin is a regulator of phosphatidylinositol-4-OH kinase. Nat. Cell Biol. *1*, 234–241.

Jones, L.P., DeMaria, C.D., and Yue, D.T. (1999). N-type calcium channel inactivation probed by gating-current analysis. Biophys. J. *76*, 2530–2552.

Jovanovic, J.N., Czernik, A.J., Fienberg, A.A., Greengard, P., and Sihra, T.S. (2000). Synapsins as mediators of BDNF-enhanced neurotransmitter release. Nat. Neurosci. *3*, 323–329.

Koester, H.J., and Sakmann, B. (2000). Calcium dynamics associated with action potentials in single nerve terminals of pyramidal cells in layer 2/3 of the young rat neocortex. J. Physiol. *529*, 625–646.

Korte, M., Carroll, P., Wolf, E., Brem, G., Thoenen, H., and Bonhoeffer, T. (1995). Hippocampal long-term potentiation is impaired in mice lacking brain-derived neurotrophic factor. Proc. Natl. Acad. Sci. USA *92*, 8856–8860.

Lee, A., Wong, S.T., Gallagher, D., Li, B., Storm, D.R., Scheuer, T., and Catterall, W.A. (1999). Ca2+/calmodulin binds to and modulates P/Q-type calcium channels. Nature *399*, 155–159.

Lin, L.F., Doherty, D.H., Lile, J.D., Bektesh, S., and Collins, F. (1993). GDNF: a glial cell line-derived neurotrophic factor for midbrain dopaminergic neurons. Science *260*, 1130–1132.

Liou, J.C., and Fu, W.M. (1997). Regulation of quantal secretion from developing motoneurons by postsynaptic activity-dependent release of NT-3. J. Neurosci. *17*, 2459–2468.

Llinas, R. (1982). Calcium in synaptic transmission. Sci. Am. *247*, 56–65.

Lohof, A.M., Ip, N.Y., and Poo, M.M. (1993). Potentiation of developing neuromuscular synapses by the neurotrophins NT-3 and BDNF. Nature *363*, 350–353.

Lu, B., and Chow, A. (1999). Neurotrophins and hippocampal synaptic plasticity. J. Neurosci. Res. *58*, 76–87.

Maffei, L., Berardi, N., Domenici, L., Parisi, V., and Pizzorusso, T. (1992). Nerve growth factor (NGF) prevents the shift in ocular dominance distribution of visual cortical neurons in monocularly deprived rats. J. Neurosci. *12,* 4651–4662.

McAllister, A.K., Lo, D.C., and Katz, L.C. (1995). Neurotrophins regulate dendritic growth in developing visual cortex. Neuron *15*, 791–803.

McAllister, A.M., Katz, L.C., and Lo, D.C. (1999). Neurotrophins and synaptic plasticity. Annu. Rev. Neurosci. *22*, 295–318.

Ming, G.-L., Henley, J., Tessier-Lavigne, M., Song, H.-J., and Poo, M.-M. (2001). Electrical activity modulates growth cone guidance by diffusible factors. Neuron *29*, 441–451.

Nguyen, Q.T., Parsadanian, A.S., Snider, W.D., and Lichtman, J.W. (1998). Hyperinnervation of neuromuscular junctions caused by GDNF overexpression in muscle. Science *279*, 1725–1729.

Nick, T.A., and Ribera, A.B. (2000). Synaptic activity modulates presynaptic excitability. Nat. Neurosci. *3*, 142–149.

Olafsson, P., Wang, T., and Lu, B. (1995). Molecular cloning and

functional characterization of the Xenopus Ca^{2+}-binding protein frequenin. Proc. Natl. Acad. Sci. USA *92,* 8001–8005.

Oppenheim, R.W., Houenou, L.J., Johnson, J.E., Lin, L.F., Li, L., Lo, A.C., Newsome, A.L., Prevette, D.M., and Wang, S. (1995). Developing motor neurons rescued from programmed and axotomy-induced cell death by GDNF. Nature *373,* 344–346.

Pachnis, V., Mankoo, B., and Constantini, F. (1993). Expression of the c-ret proto-oncogene during mouse embryogenesis. Development *119,* 1005–1007.

Paterlini, M., Revilla, V., Grant, A.L., and Wisden, W. (2000). Expression of the neuronal calcium sensor protein family in the rat brain. Neuroscience *99,* 205–216.

Patterson, S.L., Abel, T., Deuel, T.A., Martin, K.C., Rose, J.C., and Kandel, E.R. (1996). Recombinant BDNF rescues deficits in basal synaptic transmission and hippocampal LTP in BDNF knockout mice. Neuron *16,* 1137–1145.

Peterson, B.Z., DeMaria, C.D., Adelman, J.P., and Yue, D.T. (1999). Calmodulin is the Ca2+ sensor for Ca2+-dependent inactivation of L-type calcium channels. Neuron *22,* 549–558.

Pongs, O., Lindemeier, J., Zhu, X.R., Theil, T., Engelkamp, D., Krah-Jentgens, I., Lambrecht, H.-G., Koch, K.W., Schwemer, J., Rivosecchi, R., et al. (1993). Frequenin-A novel calcium-binding protein that modulates synaptic efficacy in the *Drosophila* nervous system. Neuron *11,* 15–28.

Pozzo-Miller, L., Gottschalk, W.A., Zhang, L., McDermott, K., Du, J., Gopalakrishnan, R., Oho, C., Shen, Z., and Lu, B. (1999). Impairments in high frequency transmission, synaptic vesicle docking and synaptic protein distribution in the hippocampus of BDNF knockout mice. J. Neurosci. *19,* 4972–4983.

Rutherford, L.C., Nelson, S.B., and Turrigiano, G.G. (1998). BDNF has opposite effects on the quantal amplitude of pyramidal neuron and interneuron excitatory synapses. Neuron *21,* 521–530.

Ryan, T.A., Reuter, H., Wendland, B., Schweizer, F.E., Tsien, R.W., and Smith, S.J. (1993). The kinetics of synaptic vesicle recycling measured at single presynaptic boutons. Neuron *11,* 713–724.

Stoop, R., and Poo, M.M. (1995). Potentiation of transmitter release by ciliary neurotrophic factor requires somatic signaling. Science *267,* 695–699.

Treanor, J.J., Goodman, L., de Sauvage, F., Stone, D.M., Poulsen, K.T., Beck, C.D., Gray, C., Armanini, M.P., Pollock, R.A., Hefti, F., et al. (1996). Characterization of a multicomponent receptor for GDNF. Nature *382,* 80–83.

Vicario-Abejon, C., Collin, C., McKay, R.D., and Segal, M. (1998). Neurotrophins induce formation of functional excitatory and inhibitory synapses between cultured hippocampal neurons. J. Neurosci. *18,* 7256–7271.

Wang, X.H., and Poo, M.M. (1997). Potentiation of developing synapses by postsynaptic release of neurotrophin-4. Neuron *19,* 825–835.

Wang, T., Xie, K.W., and Lu, B. (1995). Neurotrophins promote maturation of developing neuromuscular synapses. J. Neurosci. *15,* 4796–4805.

Wiedemann, C., Schafer, T., Burger, M.M., and Sihra, T.S. (1998). An essential role for a small synaptic vesicle-associated phosphatidylinositol 4-kinase in neurotransmitter release. J. Neurosci. *18,* 5594–5602.

Xie, Z.P., and Poo, M.M. (1986). Initial events in the formation of neuromuscular synapse: rapid induction of acetylcholine release from embryonic neuron. Proc. Natl. Acad. Sci. USA *83,* 7069–7073.

Xie, K., Wang, T., Olafsson, P., Mizuno, K., and Lu, B. (1997). Activity-dependent expression of NT-3 in muscle cells in culture: implication in the development of neuromuscular junctions. J. Neurosci. *17,* 2947–2958.

Xu, B., Gottschalk, W., Chow, A., Wilson, R.I., Schnell, E., Zang, K., Wang, D., Nicoll, R.A., Lu, B., and Reichardt, L.F. (2000). The role of brain-derived neurotrophic factor receptors in the mature hippocampus: modulation of long-term potentiation through a presynaptic mechanism involving TrkB. J. Neurosci. *20,* 6888–6897.

Yan, Q., Matheson, C., and Lopez, O.T. (1995). In vivo neurotrophic

effects of GDNF on neonatal and adult facial motor neurons. Nature *373,* 341–344.

Yang, F., He, X., Feng, L., Mizuno, K., Liu, X., Russell, J., Xiong, W., and Lu, B. (2001). PI3 kinase and IP3 are both necessary and sufficient to mediate NT3-induced synaptic potentiation. Nat. Neurosci. *4,* 19–28.

Yazejian, B., DiGregorio, D.A., Vergara, J.L., Poage, R.E., Meriney, S.D., and Grinnell, A.D. (1997). Direct measurements of presynaptic calcium and calcium-activated potassium currents regulating neurotransmitter release at cultured Xenopus nerve-muscle synapses. J. Neurosci. *17,* 2990–3001.

Zhao, Y., and Szaro, B.G. (1997). Xefiltin, a new low molecular weight neuronal intermediate filament protein of Xenopus laevis, shares sequence features with goldfish gefiltin and mammalian alpha-internexin and differs in expression from XNIF and NF-L. J. Comp. Neurol. *377,* 351–364.

Zhao, M., Hollingworth, S., and Baylor, S.M. (1996). Properties of tri- and tetracarboxylate Ca2+ indicators in frog skeletal muscle fibers. Biophys. J. *70,* 896–916.

Zucker, R.S. (1989). Short-term synaptic plasticity. Ann. Rev. Neurosci. *12,* 13–31.

Zuhlke, R.D., Pitt, G.S., Deisseroth, K., Tsien, R.W., and Reuter, H. (1999). Calmodulin supports both inactivation and facilitation of L-type calcium channels. Nature *399,* 159–162.